DOI: https://doi.org/10.62985/j.huit_ojs.vol24.no1.28

OPERATION OF FLYING-CAPACITOR MODULAR MULTILEVEL CONVERTER WITH FOUR-WINDING COUPLED INDUCTORS

Van Tan Luong*, Le Duc Dung, Huynh Nhat Quang

Ho Chi Minh City University of Industry and Trade

*Email: *luongvt@huit.edu.vn*

Received: 22 December 2023; Accepted: 28 February 2024

ABSTRACT

In this paper, a coupled inductor with four windings for a flying-capacitor modular multilevel converter (FC-MMC) has been proposed to reduce the volume and weight of the magnetic component. In the conventional flying-capacitor MMC, four discrete inductors are needed to be assembled for a leg, however, these four inductors can be reduced to only one. By this, the volume of the magnetic core can be reduced by 47.3% and 8.2%, respectively, compared with the discrete and two-winding coupled inductors. The performance of the FC-MMC with the proposed coupled inductor has been shown by the simulation results.

Keywords: Coupled inductor, flying-capacitor modular multilevel converters, medium-voltage motor drive, submodule capacitor voltage ripple.

1. INTRODUCTION

Recently, MMC is regarded as one of the promising topologies for the medium/high-voltage applications due to its merits of low output voltage harmonics, modularity, scalability, and ability of fault-tolerant operation [1]. However, one of the main issues of the MMC-fed motor drives is that the submodule (SM) capacitor voltage fluctuations are proportional to the output current and inversely proportional to the fundamental frequency [2-4]. Therefore, the operating speed region of the motor is limited. To overcome this issue, several studies have been performed [2-10].

In [2, 3], the capacitor voltage fluctuations at a low-speed operation can be suppressed by the injection of the high-frequency common-mode voltage (CMV) and circulating current in the leg. This control method can alleviate the SM capacitor voltage fluctuations significantly, but the CMV issue appears in the motor side. It leads to the premature failure of winding insulation and motor bearing. In [4], a flying-capacitor (FC) MMC has been proposed to mitigate the SM capacitor voltage fluctuations without injecting the high-frequency CMV. Thus, the CMV does not exist on the motor side. However, twelve discrete inductors are assembled in this topology. To reduce the volume, weight and cost of the magnetic cores, the two-winding coupled inductor was proposed previously [10]. However, the magnetic core can be reduced further for the FC-MMC.

In this paper, utilization of four-winding (4W) coupled inductor is proposed for the FC-MMC. Since one coupled inductor covers a leg, only three coupled inductors are needed for the three-phase FC-MMC. It is noted that the volume of the 4W coupled inductor can be reduced by 47.3% and 8.2%, respectively, compared with the discrete and two-winding coupled inductors. The validity of the proposed topology is verified by simulation results for a 4160-V / 1-MW IM drive system.

2. FLYING-CAPACITOR MMC WITH FOUR-WINDINGS COUPLED INDUCTORS

2.1. Circuit structure

Figure 1(a) shows the circuit configuration of the FC-MMC, which consists of three legs (*x: a, b, c*). In one leg, there are an upper arm, a lower arm, and a flying-capacitor branch. Each arm can be regarded as a combination of two half-arms. Besides, a flying capacitor, C_F, is used to link the middle taps of the upper and lower arms in a leg. In the conventional flying-capacitor MMCs, one discrete inductor is employed in each half-arm to reduce the switching current. However, four discrete inductors in one leg can be substituted by a coupled inductor with four windings to mitigate the switching current as well as to reduce the volume and weight of the system.

A per-phase equivalent circuit of a leg is shown in Figure 1(b), where the voltages and currents of four half-arms are expressed as

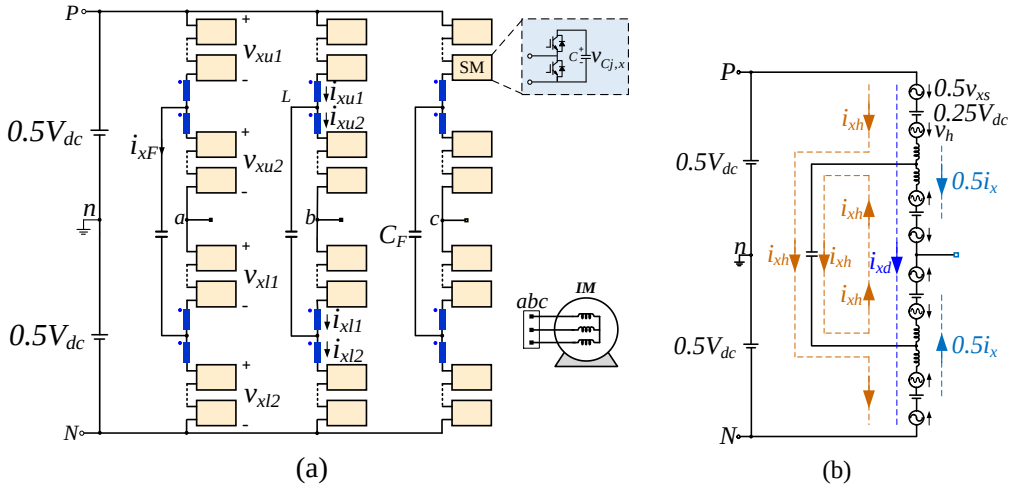

Figure 1. Flying-capacitor MMC. (a) Circuit configuration. (b) Per-phase equivalent circuit of a leg.

$$\begin{cases} v_{xu1} = 0.25V_{dc} - 0.5v_{xs} - v_h \\ v_{xu2} = 0.25V_{dc} - 0.5v_{xs} + v_h \\ v_{xl1} = 0.25V_{dc} + 0.5v_{xs} - v_h \\ v_{xl2} = 0.25V_{dc} + 0.5v_{xs} + v_h \end{cases}, \tag{1}$$

$$\begin{cases} i_{x1} = i_{xd} + 0.5i_x + i_{xh} \\ i_{x2} = i_{xd} + 0.5i_x - i_{xh} \\ i_{x3} = i_{xd} - 0.5i_x - i_{xh} \\ i_{x4} = i_{xd} - 0.5i_x + i_{xh} \end{cases}, \tag{2}$$

where V_{dc}, v_{xs}, v_h i_{xd}, i_x and i_{xh} are the DC-link voltage, phase voltage, high-frequency voltage, DC component of the circulating current flowing in the leg, AC output current and high-frequency circulating current component, respectively.

2.2. Proposed magnetic integration scheme

Figure 2(a) and (b) demonstrate the discrete inductor and two-winding coupled inductor, respectively, which are used for the FC-MMC [4, 10]. If the coupled inductor is wound with four windings as shown in Figure 2(c), the volume and weight of the magnetic core can be further reduced.

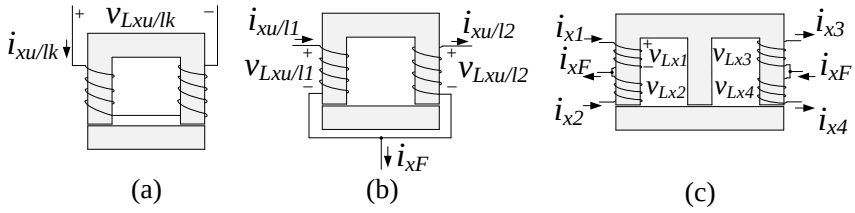

Figure 2. Schematic representation of inductors. (a) Discreate inductor. (b) two-winding inductor. (c) four-winding inductor.

In the 4W coupled inductor, the voltages in each half-arm are expressed as

$$\begin{bmatrix} v_{Lx1} \\ v_{Lx2} \\ v_{Lx3} \\ v_{Lx4} \end{bmatrix} = \begin{bmatrix} L_1 & M_{12} & M_{13} & M_{14} \\ M_{12} & L_2 & M_{23} & M_{24} \\ M_{13} & M_{23} & L_3 & M_{34} \\ M_{14} & M_{24} & M_{34} & L_4 \end{bmatrix} \begin{bmatrix} \dot{i}_{x1} \\ \dot{i}_{x2} \\ \dot{i}_{x3} \\ \dot{i}_{x4} \end{bmatrix}, \tag{3}$$

where L_i represents the self-inductance of winding i (L_1=L_2=L_3=L_4=L) and M_{ij} is the mutual inductance between windings i and j which is given by

$$M_{ij} = k_{ij}\sqrt{L_i L_j}\,. \tag{4}$$

Substituting (2) and (4) into (3) yields

$$\begin{cases} v_{Lx1} = L\left[(1-k_{12})(\dot{i}_{xd}+0.5\dot{i}_x)+(k_{13}-k_{14})(\dot{i}_{xd}-0.5\dot{i}_x)+(1+k_{12}-k_{13}-k_{14})\dot{i}_{xh}\right] \\ v_{Lx2} = L\left[(1-k_{12})(\dot{i}_{xd}+0.5\dot{i}_x)+(k_{23}-k_{24})(\dot{i}_{xd}-0.5\dot{i}_x)-(1+k_{12}-k_{23}-k_{24})\dot{i}_{xh}\right] \\ v_{Lx3} = L\left[(1-k_{34})(\dot{i}_{xd}+0.5\dot{i}_x)+(k_{13}-k_{23})(\dot{i}_{xd}-0.5\dot{i}_x)-(1+k_{34}-k_{13}-k_{23})\dot{i}_{xh}\right] \\ v_{Lx4} = L\left[(1-k_{34})(\dot{i}_{xd}+0.5\dot{i}_x)+(k_{14}-k_{24})(\dot{i}_{xd}-0.5\dot{i}_x)+(1+k_{34}-k_{14}-k_{24})\dot{i}_{xh}\right] \end{cases}. \tag{5}$$

In order to design the magnetic component, the effective inductance for the high-frequency circulating current, i_{xh}, is taken into account to prevent high di/dt. The effective inductances for the output current, i_x, can be neglected owing to leakage inductances of induction motor itself. Thus, the effective inductances for the high-frequency circulating current in four half-arms, L_{xhi}, are expressed as

$$\begin{cases} L_{xh1} = L(1+k_{12}-k_{13}-k_{14}) \\ L_{xh2} = L(1+k_{12}-k_{23}-k_{24}) \\ L_{xh3} = L(1+k_{34}-k_{13}-k_{23}) \\ L_{xh4} = L(1+k_{34}-k_{14}-k_{24}) \end{cases}. \tag{6}$$

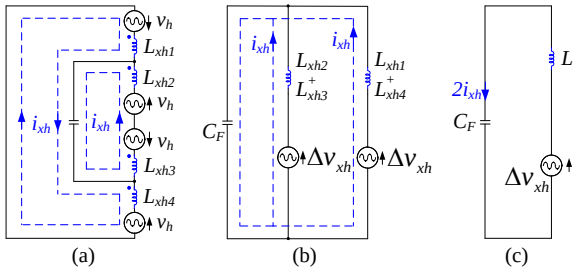

Figure 3. High-frequency equivalent circuit of single-phase FC-MMC. (a) High-frequency equivalent circuit per phase. (b) Simplified circuit with Δv_{xh} in two arms. (c) Simplified circuit.

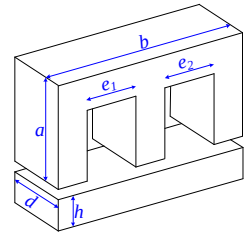

Figure 4. Magnetic core.

With the calculated L_{xhi} for half-arms, the high-frequency equivalent circuit for a single phase is shown in Figure 3(a). Then, it is simplified to Figure 3(b), where the high-frequency voltage compensation, Δv_{xh}, is used to control i_{xh}. For a high performance of the FC-MMC, the injected frequency, f_h, should be equal to the resonant frequency to minimize the impedance of the equivalent *LC* circuit. Thus, in Figure 3(b), the inductance value of L_{xh2} + L_{xh3} is equal to that of L_{xh1} + L_{xh4}, which leads to $k_{14} = k_{23}$. Besides, the injected frequency should not be sensitive to the coupling coefficients. It means that

$$\begin{cases} k_{12} = k_{13} + k_{14} = k_{23} + k_{24} \\ k_{34} = k_{12} = k_{13} + k_{24} = k_{14} + k_{24} \end{cases}. \tag{7}$$

This is the case that the windings 1 and 2 are placed symmetrically to windings 3 and 4, which is shown in Figure 2(c).

Finally, the high-frequency equivalent circuit is simplified to Figure 3(c), which consists of *L* and C_F components. From this, the resonant frequency can be calculated. It means that the flying capacitance, C_F, is kept like that of the conventional FC-MMC in spite of integration of 4W coupled inductors.

2.3. Inductor design

To compare the volumes of inductors, the parameters for the down-scaled prototype are considered [10]. The effective inductance applied to the high-frequency circulating current component is 2 mH in a half-arm. The maximum currents of inductors, I_{max}, are obtained from the superposition of the maximum values of the currents which flow through each core, where i_{xd_max} = 4 A, i_{x_max} = 16 A and i_{xh_max} = 20 A. Thus, I_{max} of the discrete inductor, two-winding coupled inductor and 4W coupled inductor are 32 A, 20 A and 20 A, respectively. The area-product method [11] is applied to select magnetic cores of inductors. The core material is silicon steel (7.65 g/cm^3) and the windings (8.9 g/cm^3) are of the rectangular type of wire with AIW coating. In cases of discrete and two-winding coupled inductor, core type is UI, whereas, in case of 4W coupled inductor, core type is EI shown in Figure 4. A comparison of volume and weight of inductors is shown in Table 1. It is noted that the 4W coupled inductor is 47.3% smaller in volume and 47.5% lighter in weight compared with the discrete inductors. Compared with the two-winding coupled inductor, the volume and weight can be reduced by 8.2% and 8.6%, respectively.

Table 1. Comparison of volume and weight of inductors

Parameter	Discrete	Two-winding	Four-winding
Coil turns (*N*)	88	64	64
a [cm]	8	10	4
b [cm]	6	6	22
d [cm]	5	5	5
h [cm]	2	2	2
e_1 [cm]	2	2	8
e_2 [cm]	-	-	8
Total volume of core and winding [cm^3]	1277	732	672
Total weight of core and winding [kg]	10.1	5.8	5.3

3. SIMULATION RESULTS

Table 2. Systems parameters and ratings

Parameters	Symbol	Value
Converter (MMC)		
Apparent power (kVA)	S	1081
DC-link voltage (V)	V_{dc}	7000
Coupling coefficient (coil 1-2, 3-4)	k_{12}, k_{34}	0.9
Coupling coefficient (coil 1-3, 2-4)	k_{13}, k_{24}	0.45
Number of SMs per arm	N	4
SM capacitor voltage reference (V)	v_c^*	1750
Half-arm inductance (mH)	L	2
SM capacitance (mF)	C	3.5
Flying capacitance (mF)	C_F	1
Carier frequency (Hz)	f_c	2000
Injected frequency (Hz)	f_h	112.5
Induction Motor (IM)		
Output power (hp)	P_o	1250
Rated voltage (V)	V_{LL}	4160
Rated current (A)	I_{rated}	150
Rated speed (rpm)	ω_{rm_rated}	1189
Rated torque (N.m)	T_{rated}	7490

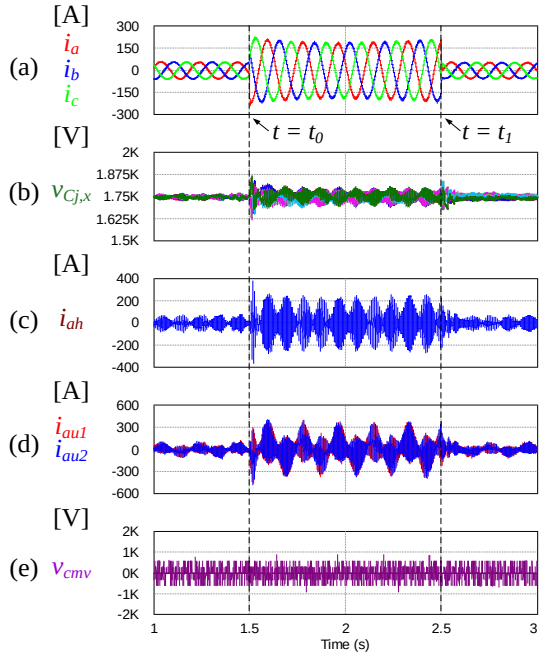

Figure 5. Performance at low-speed operation (ω_{rm} = 100 rpm) under load change condition. (a) Output current. (b) SM capacitor voltages. (c) High-frequency circulating current. (d) Top and bottom half-arm currents. (e) Common-mode voltage.

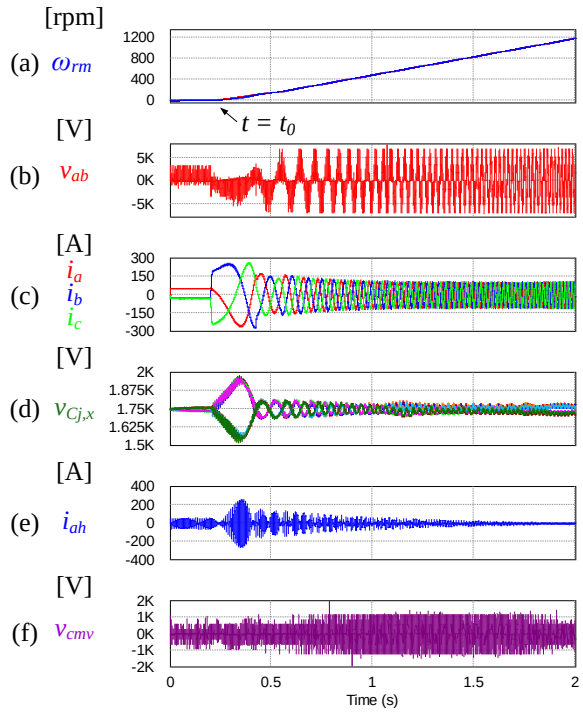

Figure 6. Performance of accelerating process from zero to rated speed.
(a) Motor speed. (b) Line-to-line voltage. (c) Output current. (d) SM capacitor voltages.
(e) High-frequency circulating current. (f) Common-mode voltage.

To verify the effectiveness of the proposed 4W coupled inductor, a 4160-V / 1-MW FC-MMC system with four SMs per arm has been modeled for simulation. The parameters and ratings of MMC and induction motor are listed in Table 2.

Figure 5 illustrates the performance of the FC-MMC with 4W coupled inductors at low-speed operation (ω_{rm} = 100 rpm) when the load torque is changed from no load to full load and back to no load at $t = t_0$ and $t = t_1$, respectively. Figure 5(a) shows the three-phase output currents (i_a, i_b and i_c), where they are well balanced at both the transient and steady states. The SM capacitor voltages are shown in Figure 5(b), where they are well controlled to follow the reference v_c^* (1750 V). Figure 5(c) shows the high-frequency circulating current, i_{ah}, which consists of the injected frequency component (f_h = 112.5 Hz) besides the fundamental one (f_o = 5 Hz). At full load, the amplitude of i_{xh} is increased in order to redistribute the imbalanced power between upper and lower arms. The top and bottom half-arm currents (i_{au1} and i_{au2}) in the upper arm and CMV are shown in Figure 5(d) and (e), respectively.

Figure 6 shows the system performance during acceleration from zero at $t = t_0$ to the rated speed under no load condition. Figure 6(a) illustrates the motor speed, ω_{rm}, which is accelerated from 0 to 1189 rpm. The line-to-line output voltage, v_{ab}, and three-phase output currents are shown in Figure 6(b) and (c), respectively, where the fundamental frequency is increased from 0 Hz to 60 Hz. The SM capacitor voltages, which are shown in Figure 6(d), are well balanced at 1750 V. The high-frequency circulating current of phase-*a* is shown in Figure 6(e), which is decreased as the motor speed is increased. The CMV is shown in Figure 6(f).

Figure 7 illustrates the inductor voltage waveforms in four half-arms, where v_{Lxi_mes} is the measured voltage and v_{Lxi_cal} is the calculated one from (3)-(5). As mentioned in (5), the effective inductances for i_{xd} and i_x are small compared with that for i_{xh}. Thus, the inductor voltages consist of the injected frequency component, f_h, additional to the switching frequency.

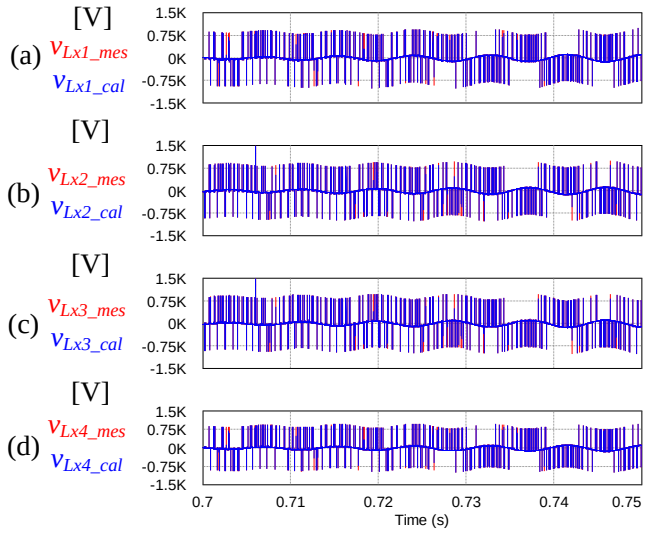

Figure 7. Inductor voltage waveforms in four half-arms.

4. CONCLUSION

This paper has proposed an FC-MMC with the four-winding coupled inductor for the induction motor drives systems in order to reduce the volume and weight of the magnetic component. With the proposed method, the volume of the inductor can be reduced by 47.3% and 8.2%, respectively, compared with the discrete and two-winding coupled inductors. The feasibility of the 4W coupled inductor has been confirmed by the simulation results for a 4160-V / 1-MW IM drive system.

REFERENCES

1. Lesnicar A. and Marquardt R. - An innovative modular multilevel converter topology suitable for a wide power range, in 2003 IEEE Bologna PowerTech **3** (2003) 272-277, DOI: 10.1109/PTC.2003.1304403.
2. Korn A. J., Winkelnkemper M., and Steimer P. - Low output frequency operation of the modular multi-level converter, in Proceedings *under* IEEE Energy Conversion Congress and Exposition (2010) 3993-3997, DOI: 10.1109/ECCE.2010.5617802.
3. Hagiwara M., Hasegawa I., and Akagi H., -Start-up and low-speed operation of an electric motor driven by a modular multilevel cascade inverter, IEEE Transactions on Industry Applications **49** (4) (2013) 1473–1480, DOI: 10.1109/TIA.2013.2256331.
4. Du S., Wu B., Zargari N. R., and Cheng Z. - A flying-capacitor modular multilevel converter for medium-voltage motor drive, IEEE Transactions on Power Electronics **32** (3) (2017) 2081-2089, DOI: 10.1109/TPEL.2016.2565510.
5. Le D. D. and Lee D.-C. - A modular multilevel converter topology with novel middle submodules to reduce capacitor voltage fluctuations, IEEE Transactions on Power Electronics **37** (1) (2022) 70-75, DOI: 10.1109/TPEL.2021.3101884.
6. Antonopoulos A., Ängquist L., Norrga S., Ilves K., Harnefors L., and Nee H. P. - Modular multilevel converter AC motor drives with constant torque from zero to nominal speed, IEEE Transactions on Industry Applications **50** (3) (2014) 1982-1993, DOI: 10.1109/TIA.2013.2286217.

7. Antonopoulos A., Ängquist L., Harnefors L., and Nee H. P. - Optimal selection of the average capacitor voltage for variable-speed drives with modular multilevel converters, IEEE Transactions on Power Electronics **30** (1) (2015) 227-234 DOI: 10.1109/TPEL.2014.2316273.
8. Le D. D. and Lee D.-C. - Current stress reduction and voltage THD improvement of FC-MMCs for AC machine drive applications, IEEE Transactions on Industrial Electronics **69** (1) (2022) 90-100, DOI: 10.1109/TIE.2021.3050394.
9. Zhao F., Xiao G., Zhu T., Zheng X., Wu Z., and Zhao T. - A coordinated strategy of low-speed and start-up operation for medium-voltage variable-speed drives with a modular multilevel converter, IEEE Transactions on Power Electronics **35** (1) (2020) 709-724, DOI: 10.1109/TPEL.2019.2913696.
10. Le D. D., Lee D.-C., and Kim H.-G. - Three-phase flying-capacitor MMC with six coupled inductors, Journal Power Electronics **20** (4) (2000) 916-925, DOI: 10.1007/s43236-020-00099-3.
11. McLyman C. W. T. - Transformer and inductor design handbook. CRC Press, chapter 10 (2011), DOI: 10.1201/b10865.

TÓM TẮT

BỘ BIẾN ĐỔI ĐA BẬC CẤU HÌNH MÔ-ĐUN TỤ ĐIỆN BAY VỚI CUỘN CẢM KẾT NỐI BỐN CUỘN DÂY

Văn Tấn Lượng*, Lê Đức Dũng, Huỳnh Nhật Quang

Trường Đại học Công Thương Thành phố Hồ Chí Minh

*Email: *luongvt@huit.edu.vn*

Trong bài báo này, cuộn cảm kết nối với bốn cuộn dây cho bộ biến đổi đa bậc cấu hình mô-đun tụ điện bay (FC-MMC) đã được đề xuất để giảm thể tích và trọng lượng của thành phần từ tính. Đối với bộ FC-MMC thông thường, bốn cuộn cảm rời rạc cần phải lắp ráp cho một pha. Tuy nhiên, bốn cuộn cảm này có thể được thay thế bằng cách thiết kế một cuộn cảm kết nối với bốn cuộn dây. Bằng cách này, thể tích của lõi từ có thể giảm lần lượt là 47,3% và 8,2% so với các cuộn cảm rời rạc và cuộn cảm kết nối hai cuộn dây. Tính khả thi của phương pháp đề xuất đã được xác minh bằng kết quả mô phỏng cho hệ thống truyền động động cơ 4160-V/1-MW với cuộn cảm kết nối được sử dụng trong cấu hình của FC-MMC.

Từ khóa: Cuộn cảm kết nối, bộ biến đổi đa bậc cấu hình mô-đun tụ điện bay, hệ truyền động với động cơ trung thế, dao động điện áp trên tụ của mô-đun.